Measurement of AC Loss and Magnetic Field during Ramps in the LHC Model Dipoles

Z. Ang, I. Bejar, L. Bottura, D. Richter, M. Sheehan, L. Walckiers, R. Wolf
CERN, CH-1211 Geneva 23, Switzerland

Abstract — **We describe the systems for AC loss and magnetic field measurements developed for the LHC superconducting magnets. AC loss measurements are performed using an electric method, while field measurements are performed using either fixed pick-ups or rotating coils. We present results obtained on 1-m long model dipoles, and compare the results of the different methods in terms of average inter-strand resistance.**

I. Introduction

The LHC Large Hadron Collider will accelerate proton beams from an injection energy around 450 GeV to the nominal coast value of 7 TeV. The superconducting magnets, operated in superfluid helium and forming the main part of the LHC ring, will need to be cycled in accordance to maintain the bending and focussing strength required. In particular, the main arc dipole magnets receive the beam at the injection field of 0.54 T, and follow its acceleration up to the nominal operating field of 8.36 T in approximately 20 minutes. The corresponding field and current ramp-rates are modest, 6.5 mT/s and 10 A/s respectively. It is nevertheless of vital importance to control field distortions caused by cable coupling currents to achieve tight control of the LHC beam during the beginning of the acceleration[1]. In addition, AC loss should be limited to avoid performance limitations during ramps and to minimize the cryogenic load. To limit cable coupling currents an inter-strand resistance target of 15 μΩ has been set, with a spread of less than 5 μΩ within the winding cross section. This range of inter-strand resistance guarantees that AC loss is negligible and that field distortions are small. A slow ramp at the beginning of the beam acceleration is an additional mean that we envisage to avoid detrimental effects on the beam[2].

This paper describes the systems that we have developed to measure the AC loss, the main magnetic field component and the higher order harmonics during operating current ramps. We concentrate in particular on tests performed on a series of 1-m long dipole models described elsewhere[3]. We finally give a summary of measurement results in terms of inter-strand contact resistance and measured field distortion.

II. Measurement Systems

A. Test Set-up

The measurements of the dipole model magnets are performed in a vertical test set-up, shown in Fig. 1. The magnet is suspended inside the cryostat. A *λ-plate* separates the pool boiling helium bath from the superfluid bath, both at atmospheric pressure (Claudet bath). The subcooled superfluid state in the lower portion of the cryostat is achieved by means of a heat exchanger, where saturated superfluid helium conditions are obtained via Joule-Thomson expansion of liquid helium from 1 bar down to approximately 15 mbar. The λ-plate has a number of leak-tight penetrations for superconducting bus-bars, instrumentation wires and a sliding bearing for the rotating shaft used for the magnetic measurements described below.

B. AC Loss

The measurement of the AC loss is based on the independent and simultaneous acquisition of the current I and the voltage V at the terminals of the magnet during trapezoidal current cycles. The loss is obtained as the time-integral of the product V×I over a closed current cycle, to cancel the contribution of the stored magnetic energy.

The electrical method is obviously sensitive to all loss contributions, including that of the joints in the coil (between layers and poles). This contribution is typically below 10 % of the total loss and is corrected in the data analysis using an average value of the total resistance obtained by an independent voltage measurement at high operating current.

The AC loss measuring system (Fig. 2) consists of six KEITHLEY Mod. 2001, $7^1/_2$ digit multimeters, controlled by a LabVIEW software running on a Pentium-90 PC. The

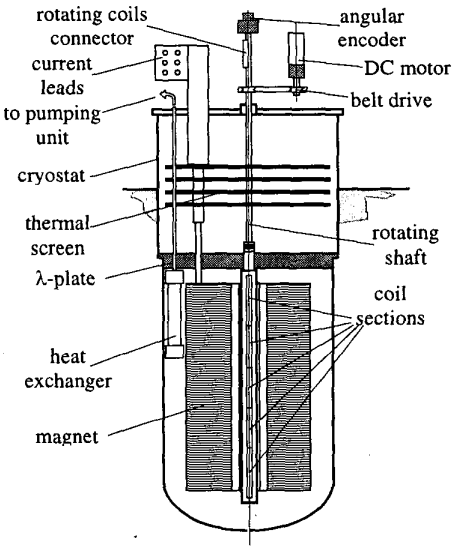

Figure 1. Schematic view of the vertical test set-up for the dipole model magnets (shown for a single aperture model).

Manuscript received September 14, 1998

multimeters are configured as integrating voltmeters synchronised by an external generator and read-out through a IEEE-488 port. Integration is needed to reject the 50 Hz and 300 Hz noise generated by the magnet power supply. A precision Direct Current Current Transformer (DCCT) mounted on the power supply generates a voltage signal proportional to the current read by the first voltmeter in the system. A second voltmeter reads the total voltage across the superconducting magnet (indicated as V1-V8 in Fig. 2). In the case of a single aperture dipole magnet the other voltmeters read the voltage of inner and outer layer of each pole. For a twin aperture magnet the voltages are read-out on the four poles forming the two apertures. These four voltage readings (indicated as V1-V2 ... V7-V8 in Fig. 2) are used for a detailed analysis of the partial loss contributions of layers and poles.

In addition to the acquisition task, the LabVIEW software controls the 20 kA, 25 V power supply, and automatically executes a sequence of ramps at increasing ramp-rate. These current cycles typically range from 0 to 6 kA with ramp-rate of 10 to 150 As^{-1}. For comparison, the nominal current for the LHC dipoles is around 11.5 kA, and the nominal ramp-rate is 10 As^{-1}. The maximum current has been restricted to 6 kA to limit the Joule heat contribution of the joints mentioned previously.

An issue that requires extreme care is the *dead-time* of the integrating voltmeters, defined as the period at the end of the integration window during which the voltmeter is blind (during count, internal data transfer and integrator reset phases). This time is typically in the range of 2 ms for the operation mode selected. The integration window is equal to 100 or 200 ms depending on the ramp-rate. Therefore the dead-time can be as much as 2 % of the window. In the presence of significant and systematic voltage spikes generated by the power supply, a dead time can degrade the accuracy of the integrated voltage.

A passive input filter with a time constant of 8 ms reduces this error so that the relative standard deviation of the measured voltage is $2 \cdot 10^{-4}$. The measurement of the current has the same accuracy for a current sweep of 6 kA. The equivalent resolution in energy dissipated over a current cycle

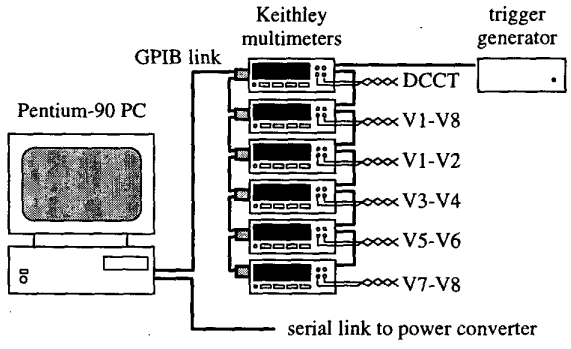

Figure 2. Block diagram of the loss measurement system. The same system configuration is used to measure the main field by means of fixed pick-ups in the magnet bore.

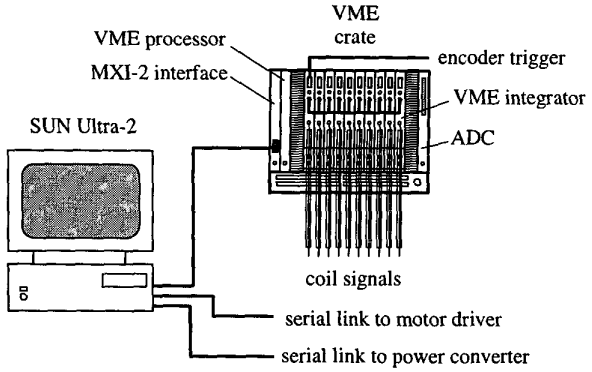

Figure 3. Block diagram of the magnetic field measurement system.

is about 4 J corresponding to $3 \cdot 10^{-4}$ of the stored energy or 8% of the dissipated energy for coils having an inter-strand resistance of 20 μΩ for ramp rates of 150 As^{-1}.

C. *Measurement of the Magnetic Field Distortion*

Quoted field harmonics are based on the following series expansion of the magnetic field in the magnet bore:

$$B_y + iB_x = B_1 \sum_{n=1}^{\infty} \frac{(b_n + ia_n)}{10^4} \left(\frac{\mathbf{z}}{R_0} \right)^{n-1} \quad (1)$$

where $\mathbf{z} = x + iy$ is the complex co-ordinate in the (x,y) coil cross sectional plane, R_0 is the reference radius (17 mm) and the coefficients b_n and a_n are the normalised multipole coefficients (expressed in so called *units*).

The measurement of the field and its harmonic components is done using radial coils mounted on a glass-fibre shaft rotating in the bore of the magnet (see Fig. 1). Five adjacent coils sections are installed to measure the field dependence along the magnet bore. Three 200 mm long coil sections cover the straight part. The 240 mm long top and bottom sections cover the magnet ends. The coils rotate in the superfluid bath. The shaft axis is held at several places, by bearings at both ends of the magnet, a sliding bearing to intercept heat conduction across the λ-plate, and a pressure tight bearing in the cryostat top flange. The magnet to λ-plate and cold-warm transitions are equipped with bellows stiff with respect to torsion but allowing axial misalignments. A DC motor mounted on the top flange of the cryostat drives the shaft via a belt transmission, while an encoder, rigidly mounted on the top end of the shaft, determines the angular position of the shaft. The typical rotation frequency is in the range of 1 Hz.

Figure 3 shows schematically the acquisition system. The voltage signals from the five rotating coils sections are read-out simultaneously by precision integrators triggered by the angular encoder. The integrated voltages are thus equal to the flux changes through the measuring coil for all angular steps, and rotation velocity variations during the measurements are compensated up to the first order. A real-time processor configures the integrators and reads the integrated voltages. Integrators and processor are mounted on a VME-bus (Versa

Module Europa, IEEE 1014-1987 standard). Overall control of the power supply, of the precision current reading, of the motor rotating the shaft and of the integrators is achieved using LabVIEW software running on a SUN Ultra-2 workstation.

We have discussed elsewhere [4] the features that allow the correct measurement of the harmonic components during current sweeps. The accuracies quoted there correspond for a 10 A/s ramp to 0.14 units of quadrupole and 0.2 units of sextupole at the reference radius of 17 mm. This accuracy is sufficient when compared to the order of magnitude of the effects measured (see later).

D. Measurement of the Main Dipole Component.

The magnetic measurement system described above does not have sufficient accuracy for the measurement of the main field with respect to the current. The reason is that in the present implementation the current reading is not synchronised with the integrator trigger provided by the angular encoder. The lack of synchronisation results in an artificial lag between current and field. To measure the contributions of coupling currents to the main field we use therefore the electronics of the AC loss system. The first voltmeter reads the current, while the remaining five voltmeters read the voltage of the same coil sections used for harmonic measurements during current ramps. In this case however the coils are kept in a fixed angular position, chosen to maximize the flux linked. The field is then obtained from the time integral of the coil voltage. The accuracy of the main field measurement with respect to static conditions is in the range of 10^{-4} T.

III. Measurement Results and Analysis

We have measured AC loss and magnetic field during ramps in 12 one meter long dipole models referred to as MBSMx magnets. The coil poles of MBSMS4 to MBSMS12 single aperture magnets and the MBSMT1 & MBSMT2 twin aperture magnets are wound in 5 blocks with a 15 mm wide Rutherford cable. The coil poles of MBSMS15 are wound in 6 blocks. Two poles are assembled in Al or SS collars to form the complete coil assembly. Details on the geometry and construction of these magnets are given elsewhere[3].

Field distortions and AC loss due to current ramps depend mainly on the inter-strand resistance R_c, or its inverse the inter-strand conductance G_c. For the ramp-rates of interest in the LHC dipoles, the coupling currents in the cables are in *resistive* regime, therefore both the AC loss and the ramp-rate dependent magnetic field contributions scale linearly with the inter-strand conductance G_c [5,6]. For a given coil geometry it is possible to calculate the AC loss and ramp-rate dependent field distortions using a detailed map of the field in the cables and assuming a G_c distribution in the coil[5]. This has been done in two cases, taking either a uniform G_c distribution in the coil, or a G_c uniform in each pole but different between poles of a coil. The result of this calculation is a set of proportionality constants for the linear scalings that relate the average G_c in the coil and the G_c in each pole to the AC loss in the whole magnet and in each pole, and to the magnetic field distortions generated during a ramp. From this analysis we have found that the contribution of the outer layer to loss and field distortions is negligible.

TABLE I. Average inter-strand resistance in the poles and average in the coil, as deduced from AC loss measurements

Magnet	Aperture	Rc pole 1 (μΩ)	Rc pole 2 (μΩ)	Rc average (μΩ)
MBSMS4		3.6	4.0	3.8
MBSMS5		2.6	3.5	3.0
MBSMS6		5.7	5.3	5.5
MBSMS7		5.7	5.8	5.7
MBSMS8		6.6	6.3	6.5
MBSMS9		6.0	6.5	6.2
MBSMS10		24	24	24
MBSMS11		28	25	26
MBSMS12		11.9	11.4	11.7
MBSMS15		18.1	17.2	17.6
MBSMT1	1	15.8	16.1	15.9
MBSMT1	2	19.7	28	23
MBSMT2	1	4.7	4.2	4.4
MBSMT2	2	9.2	7.0	7.9

We have used these scaling constants to deduce the average inter-strand resistance R_c of each pole and the average R_c in the coil from the loss measurements. The results obtained are reported in Tab. I. The cables used in the different magnets have been manufactured over a period of several years, with different surface coatings, and different heat treatments. The magnets measured are therefore not representative of a production series, and large variations of average R_c from magnet to magnet (typically from 3 to 30 μΩ) are found. On the other hand the R_c values are fairly consistent between poles and apertures of the same magnet.

In view of the LHC series measurements it is important to verify whether the ramp induced field distortions, both on main field and harmonics, could be deduced with enough accuracy from the inter-strand resistances computed from an AC loss measurements using the linear scaling discussed above. This could lead to a significant reduction and simplification of the cold tests. With this in mind we have taken the values given in Tab. I to predict ramp-rate effects on critical harmonics. The average G_c in the coil was used to compute the expected effect on the first two harmonics allowed by symmetry in a dipole, namely the dipole itself b_1 and the sextupole b_3. The G_c difference between poles has been used to predict the first harmonic resulting from a top-bottom symmetry violation, namely the skew quadrupole a_2.

In Figs. 4 to 6 we compare the measured field distortions to the predictions. We see in Fig. 4 some general agreement between expected and measured main dipole component. This agreement deteriorates as the harmonic order increases, as shown in Figs. 5 and 6 for a_2 and b_3. The disagreement in the correlation between expected and measured main field and field harmonics can be explained by two main reasons. Firstly harmonics of order higher than the dipole are increasingly sensitive to the details of the G_c distribution in

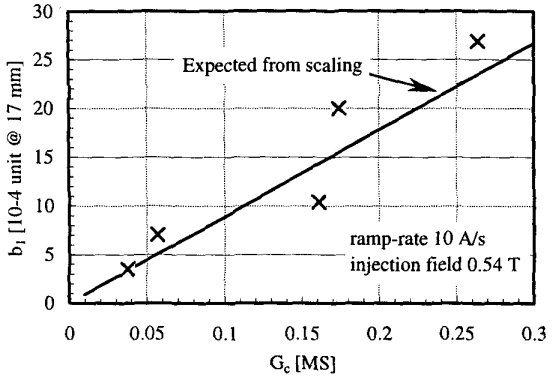

Figure 4. Measured and expected ramp-rate dependent dipole contribution based on the coil average G_c deduced from AC loss measurement.

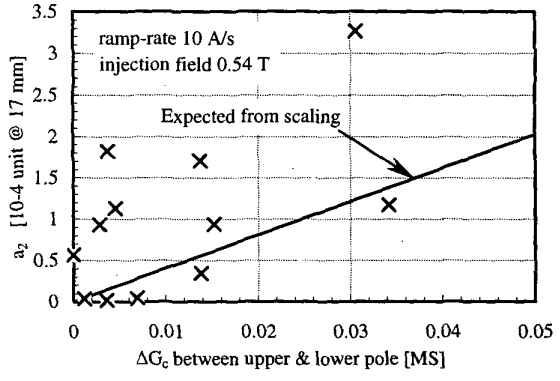

Figure 5. Measured and expected ramp-rate dependent skew quadrupole contribution based on the difference of G_c between the upper and lower poles deduced from AC loss measurement.

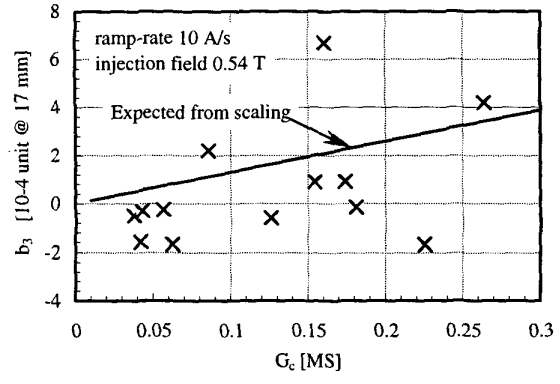

Figure 6. Measured and expected ramp-rate dependent normal sextupole contribution based on coil average G_c deduced from AC loss measurement

the coils cross section. A random G_c variation of 30 % from block to block within the coils results in random differences with respect to the homogeneous case of 9 %, 30 % and 110 % respectively for b_1, b_3, b_5. A reconstruction of the G_c distribution in a coil is indeed possible based on the measured harmonics[5,6] but was not applied here.

Secondly, both AC loss and field distortions are not only sensitive to inter-strand coupling currents, characterized by

TABLE II. ROOT MEAN SQUARE ERROR OF MEASURED FIELD HARMONICS VS. VALUES FROM AC LOSS MEASUREMENTS. THE ERRORS RELATIVE TO THE MAIN FIELD ARE IN 10^{-4} UNITS AT 17 mm RADIUS. THEY ARE GIVEN FOR THE 0.54 T INJECTION FIELD AND 6.5 mT/s (10 A/s) RAMP RATE.

b1	a2	b3	a4	b5
4.7	4.4	2.6	3.6	2

R_c, but also to inter-filament coupling currents inside the strands[7,8]. While on one side the inter-filament contribution *adds* significantly to the total AC loss (approximately 30 % of the total loss for R_c = 20 μΩ), in the case of the field distortions the inter-filament contribution is much smaller (0.7 %, 10 % and 9 % respectively for b_1, b_3, b_5) and it *subtracts* from the effect of inter-strand currents.

Table II reports a summary of the standard deviation between the measured field values and the values calculated from the average G_c or the G_c difference deduced from AC loss measurements. The errors are too large with respect to the tolerances allowed for the LHC beam [1]. Therefore we believe that we will need to characterize the magnets by means of direct field measurements in cold conditions.

IV. CONCLUSIONS

We have developed three systems to measure AC loss, main field and field harmonics in the LHC dipole magnets during current ramps. The inter-strand resistance obtained from AC loss measurements is found to correlate well with the main field component but poorly with higher order field harmonics. Based on this result we judge that the three systems deliver independent information, and will be all necessary for the series measurements of the LHC magnets.

REFERENCES

[1] L. Walckiers et al., "Towards series measurements of the LHC superconducting dipole magnets", Proc. of Particle Accelerator Conference, Vancouver, May 1997, in press.

[2] L. Bottura, A. Faus-Golfe, L. Walckiers, R. Wolf, "Field Quality of the Main Dipole Magnets for the LHC accelerator", Proc. of 1996 European Part. Acc. Conf., Sitges, 2228-2230, 1996.

[3] N. Andreev et al., "Present state of the single and twin aperture short dipole model program for the LHC", Proc. of 15th Magnet Technology Conf., Beijing, 115-118, 1997.

[4] J. Buckley, D. Richter, L. Walckiers, R. Wolf, "Dynamic Magnetic Measurements of Superconducting Magnets for the LHC", IEEE Trans. Appl. Sup., **5**, 2, 1024-1027, 1995.

[5] R. Wolf, D. Leroy, D. Richter, A. Verweij, L. Walckiers, "Determination of Inter-strand Contact Resistance from Loss and Field Measurements in LHC Dipole Prototypes and Correlation with Measurements on Cable Samples", IEEE Trans. Appl. Sup., **7**,2, 797-800, 1997.

[6] T. Ogitsu, A. Devred, V. Kovachev, "Influence of Inter-Strand Coupling Current on Field Quality of Superconducting Accelerator Magnets", Part. Acc., **57**, 215-235, 1997.

[7] A. P. Verwej, "Electrodynamics of superconducting cables in accelerator magnets", Ph. D. Thesis, Twente University, (NL), 1995.

[8] T. Ogitsu, "Influence of cable eddy currents on the magnetic field of superconducting particle accelerator magnets", Ph. D. Thesis, SSCL-N-848, Dallas, USA, 1994.